



Investigation of selective leaching conditions of ZnO, ZnFe₂O₄ and Fe₂O₃ in electric arc furnace dust in HNO₃

MERT ZORAGA, TUGBA YUCEL, SEDAT ILHAN and AHMET ORKUN KALPAKLI*

*Istanbul University—Cerrahpasa, Engineering Faculty, Metallurgical and Materials
Engineering Department, 34320, Avcilar, Istanbul, Turkey*

(Received 23 May 2020, revised 16 December, accepted 17 December 2021)

Abstract: Electric arc furnace dust (EAFD) includes mainly Zn, Fe, Pb, Ca and Mn-bearing compounds. Thus, EAFD is classified as a hazardous waste. The dissolution behavior of Zn- and Fe-bearing compounds in EAFD in nitric acid solutions was investigated in this work. The composition of Zn- and Fe-bearing compounds in the EAFD was determined as 28.58, 37.96 and 11.33 % for ZnO, ZnFe₂O₄ and Fe₂O₃, respectively. The effect of stirring speed, temperature and HNO₃ concentration on the dissolution rate of ZnO, ZnFe₂O₄ and Fe₂O₃ were investigated and optimum leaching conditions determined. While ZnO was dissolved rapidly, the dissolution rate of ZnFe₂O₄ increased with increasing temperature and HNO₃ concentration. Fe₂O₃ was not soluble in 0.5 M HNO₃ solution at 40 °C, whereas it was dissolved completely in 4 M HNO₃ solution at 80 °C.

Keywords: environmental protection; zinc recovery; leaching; zinc oxide; zinc ferrite.

INTRODUCTION

One of the most important issues with which steel producers are faced is the question of environmental protection. For example, it refers to the necessity to utilize dusts resulting from the process of steel production from scrap in electric arc furnaces, which mainly contain of Zn, Fe, Pb and a considerable amount of harmful elements, such as Cd, As, Cr and F.^{1,2} The world generation of EAFD is estimated to be around 3.7 million tons per year. Plants from Europe generate around 500.000–900.000 tons of dusts per year.¹ Turkey is Europe's 2nd and the world's 8th largest crude steel producer with an annual steel production of 37.3 million tons. While 30 % of the world's steel production (1.7 billion tons) is made in EAF as secondary production, this ratio reaches to 80 % in Turkey.

During the production of 1 ton of steel, 14–20 kg of EAFD is generated as hazardous waste. Recovery of valuable metals from EAFD is important from the

* Corresponding author. E-mail: aok13@iuc.edu.tr
<https://doi.org/10.2298/JSC200523004Z>

economic and environmental points of view. EAFD is an important source for the production of zinc and zinc-bearing chemicals for paint, rubber, natural rubber, cosmetics, stock farming, petroleum products, ceramic, glass and plating.³ The content of the main elements in EAFD varies in the range of 25–45 % of Zn, 20–35 % of Fe, 0.3–6 % of Pb, 1–10 % of Ca, 0.01–0.2 % of Cd, 0.2–0.7 % of Cr, etc., depending on the scrap processed, type of steel to be produced and operating conditions. Zinc is present in EAFD as ZnO and ZnFe₂O₄, and possibly as a complex ferrite, *e.g.*, (Zn,Mn)Fe₂O₄. ZnO is an easily workable form for both the pyrometallurgical and the hydrometallurgical method, but the ferrite form is considerably complex and difficult.^{1,4}

In the literature, different processes (hydrometallurgical or pyrometallurgical method) have been used for the processing of EAFD. The pyrometallurgical processing is usually represented by impure ZnO, which has minimal commercial value.^{5–7} This product has to be further processed by the hydrometallurgical method in order to obtain high purity zinc. Pyrometallurgical methods require some reducing agents and relatively high temperatures to produce raw zinc oxide of low commercial value.⁴ Particular attention is devoted to specific technical challenges emerging in the pyrometallurgical processing of the EAF dust and to the corresponding potential measures for improving the dust recycling by promoting the processing efficiency with the elimination of secondary hazardous pollutants.⁸ Hydrometallurgical processes are mainly based on acid (H₂SO₄, HNO₃, HCl or combined) or alkaline (usually NaOH) leaching.^{1,2,4,9–22} The alkaline leaching processes offer the potential advantage that iron remains largely insoluble. Such processes are limited, however, by their inability to recover zinc from zinc ferrite unless a reducing roast is performed first. Both approaches result in halide-containing solutions. This kind of processing is difficult.¹⁵

Caravaca *et al.* investigated the dissolution of Zn from the EAFD in basic solutions (NaOH), acidic solutions (HCl, HNO₃ and H₂SO₄) and solutions containing ammonia ((NH₄)₂SO₄, NH₄OH, NH₄Cl, (NH₄)₂CO₃) and determined that the recovery of zinc is limited when alkaline leaching is applied due to the presence of zinc ferrite. However, a relatively low iron containing leach solution is obtained.¹¹ Havlik *et al.* studied the recovery of Zn from the EAFD in H₂SO₄ solutions by the hydrometallurgical method and obtained optimum zinc leaching conditions from the EAFD at a leaching temperature of 70–90 °C and an H₂SO₄ concentration of 0.5 M.⁴ Orhan investigated leaching of EAFD in NaOH solutions and reported optimum leaching conditions, at which 85 % of Zn and 90 % of Pb were recovered, as 95 °C, 1/7 solid/liquid ratio, 10 M NaOH and a 2 h leaching time.¹⁷ Peng *et al.* used a reductive roasting method to destroy the ZnFe₂O₄ phase in order to obtain ZnO and Fe₃O₄ under a CO atmosphere and then performed leaching experiments in H₂SO₄ solution at 30–70°C. The shrinking core model was found to be the best to describe the dissolution of iron and zinc from

roasted zinc calcines at 750 °C and activation energies were calculated as 51.40 and 10.01 kJ mol⁻¹ for the leaching of Fe and Zn.²¹

The aim of this work was to investigate the dissolution behavior of ZnO, ZnFe₂O₄ and Fe₂O₃ compounds in the EAFD in HNO₃ solution and to determine the selective leaching conditions. The effect of stirring speed, HNO₃ concentration and temperature on the dissolution were determined.

EXPERIMENTAL

EAFD with a particle size fraction of -150 µm obtained from a steel company was used in the leaching experiments. X-ray fluorescence (XRF, Panalytical Axios–Minerals) and X-ray diffraction (XRD, Rigaku D/Max-2200) analyses were used for the determination of elemental and phase composition of the EAFD. SEM–EDS analyses were performed for the semi quantitative and image analysis of the EAFD and the leach residue.

Dissolution experiments were performed in a water-heated, jacketed borosilicate glass reactor (HWS DN 100, Germany) having a volume of 1 L. A thermostate with water circulation (Julabo MV4, Germany) was used to heat the reactor and to achieve isothermal conditions. The solution in the reactor was stirred with a mechanical stirrer (IKA RW 20 DZM, Germany). The solution temperature in the reactor was measured with a PT100 temperature sensor. A glass pipe including G-3 porous alumina disk at the end was used as a sampler. The dissolution experiments were performed using 5 g of the sample, 0.5–4 M HNO₃ solution, at 40–80 °C and stirring speed of 300 rpm for the determination the effect of the HNO₃ concentration, temperature and stirring speed on the dissolution behavior of the EAFD in HNO₃ solutions. In addition, the dissolution experiments of pure ZnO (Merck) and Fe₂O₃ (Merck) were also performed using 1 g of ZnO, 1 g of Fe₂O₃ (Merck), 0.5 M HNO₃ solution, at 40 °C and stirring speed of 300 rpm for the determination of the ZnO, ZnFe₂O₄ and Fe₂O₃ composition in the EAFD. When isothermal conditions were obtained, the sample weighed in a ceramic crucible was added to the reactor. Liquid samples were taken from the reactor at certain time intervals (5–180 min) and analyzed in an ICP–OES instrument.

RESULTS AND DISCUSSION

Characterization of the EAFD

The results of XRF analysis of the EAFD used in this work are given in Table I. The EAFD mainly includes oxides of Zn, Fe, Pb and Mn.

TABLE I. Chemical composition of the EAFD

Compound	ZnO	Fe ₂ O ₃	PbO	CaO	C	MnO	SiO ₂	MgO	SO ₃	Cl, F	Others ^a
Content, wt.%	41.4	36.5	4.9	3.1	3.0	2.7	1.7	1.5	2.0	0.7	< 2

^aK₂O, Al₂O₃, Cr₂O₃, CuO, P₂O₅, SnO, TiO₂, BaO, NiO, V₂O₅

The XRD diagram of the EAFD and the leach residue obtained from the experiment performed for 180 min using 0.5 M HNO₃ solution at 40 °C and a stirring speed of 300 rpm is presented in Fig. 1. It is seen from the Fig. 1a that the EAFD includes ZnFe₂O₄ (ICDD 22–1012), ZnO (ICDD 36–1451), Fe₂O₃ (ICDD 39–1346) and PbO₂ (ICDD 52–0752). ZnO was not detected in the XRD diagram (Fig. 1b) due to the rapid leaching reaction of ZnO in HNO₃ solution.

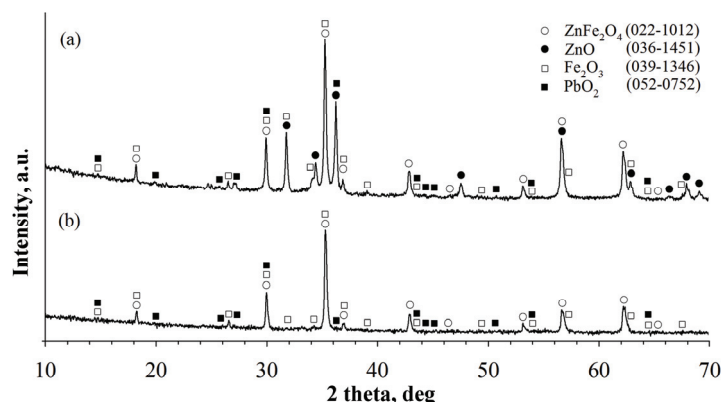


Fig 1. a) XRD diagram of the EAFD, b) the leach residue obtained from the experiment performed for 180 min using 0.5 M HNO_3 solution at 40 °C and a stirring speed of 300 rpm.

After completion of dissolution experiments, it was seen that 38 % of Fe and 86 % of Zn were extracted in the experiment performed for 180 min using 0.5 M HNO_3 solution at 40 °C (Fig. 2). It is possible to determine only the total amount of Fe and Zn in the leach solution using the ICP–OES instrument but not the exact source of Fe and Zn individually. While ZnO and ZnFe_2O_4 are sources for Zn extracted, Fe can be extracted from ZnFe_2O_4 and Fe_2O_3 .

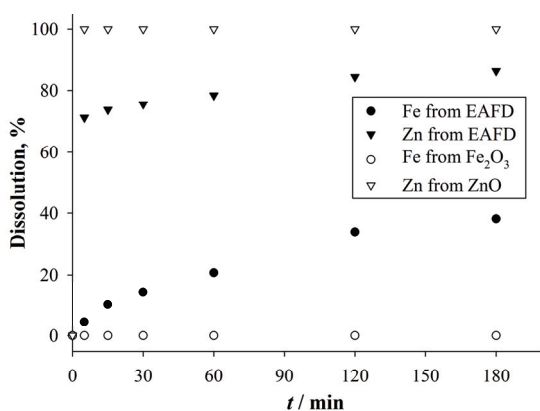


Fig. 2. Dissolution content-time diagram for Fe and Zn from the EAFD, Zn from Fe_2O_3 and Zn from ZnO . (0.5 M HNO_3 , 40 °C and 300 rpm).

The disappearance of peaks of ZnO in the XRD diagram (Fig. 1b) and the low Fe extraction rate obtained from the experiment performed at the lowest temperature (40 °C) and HNO_3 concentration (0.5 M) initiated the question of whether it is possible to determine the composition of ZnO , ZnFe_2O_4 and Fe_2O_3 in the EAFD. Therefore, two separate dissolution experiments were performed

for 180 min using 1 g of Fe_2O_3 (Merck), 1 g of ZnO (Merck), 0.5 M HNO_3 solution at 40 °C and a stirring speed of 300 rpm for the investigation of dissolution behavior of ZnO and Fe_2O_3 (Fig. 2).

ICP-OES analysis shows that ZnO was dissolved totally in 5 min of the reaction, while Fe_2O_3 was insoluble after 180 min of reaction time (no dissolved Fe was measured within the detection limit of the ICP-OES instrument). Thus, source of Fe passed to the leach solution is determined as ZnFe_2O_4 using these findings and dissolution of ZnFe_2O_4 in HNO_3 solutions.²³ It is possible to determine the composition of ZnO , ZnFe_2O_4 and Fe_2O_3 in the EAFD using the results of XRF and ICP-OES analysis as 28.58, 37.96 and 11.33 %, respectively.

Dissolution behavior of the EAFD in nitric acid solutions

Since the dissolution of ZnO in the EAFD was very rapid, the results of the dissolution experiments are presented for ZnFe_2O_4 and Fe_2O_3 as ZnFe_2O_4 dissolved, content–time and Fe_2O_3 dissolved, content–time. The dissolution, content–time diagrams are plotted using the results of the ICP-OES analysis of leach solutions taken from the reactor at defined time intervals.

The effect of stirring speed on the dissolution of EAFD

Dissolution experiments were performed using a 4 M HNO_3 solution at 80 °C for the determination of the effect of stirring speed on the dissolution rate of the EAFD in HNO_3 solutions. The ZnFe_2O_4 dissolved, content–time diagram is shown in Fig. 3.

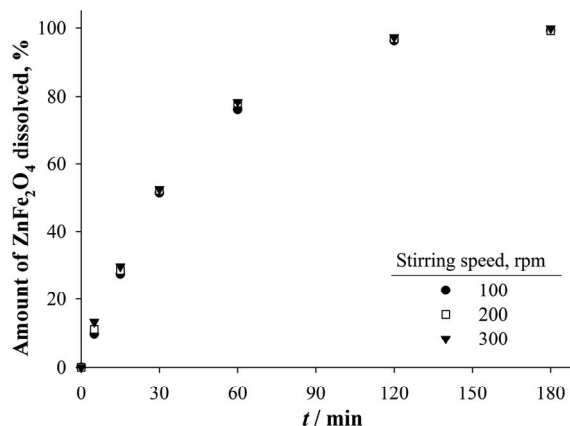


Fig. 3. ZnFe_2O_4 dissolved, content–time diagram for different stirring speeds (4 M HNO_3 and 80 °C).

As could be seen from Fig. 3, the stirring speed had no significant effect on the dissolution rate of ZnFe_2O_4 in the EAFD. Therefore, it was determined that a stirring speed of 300 rpm is adequate to eliminate the resistance of the liquid film

layer around the solid EAFD particles. Thus, a stirring speed of 300 rpm was used in all dissolution experiments.

The effect of temperature and HNO₃ concentration on the dissolution of EAFD

Dissolution experiments were performed using 0.5–4 M HNO₃ solution at temperatures of 40–80 °C and a stirring speed of 300 rpm for the determination of the effect of temperature on the dissolution rate of the EAFD in HNO₃ solutions. ZnFe₂O₄ dissolved, content-time and Fe₂O₃ dissolved, content-time diagrams are shown in Figs. 4 and 5, respectively. As seen from Fig. 4a–d, the dissolution rate of ZnFe₂O₄ increased with increasing temperature and total dissolution of ZnFe₂O₄ was obtained in the experiment performed using 4 M HNO₃ solution at 80 °C and stirring speed of 300 rpm (Fig. 4d).

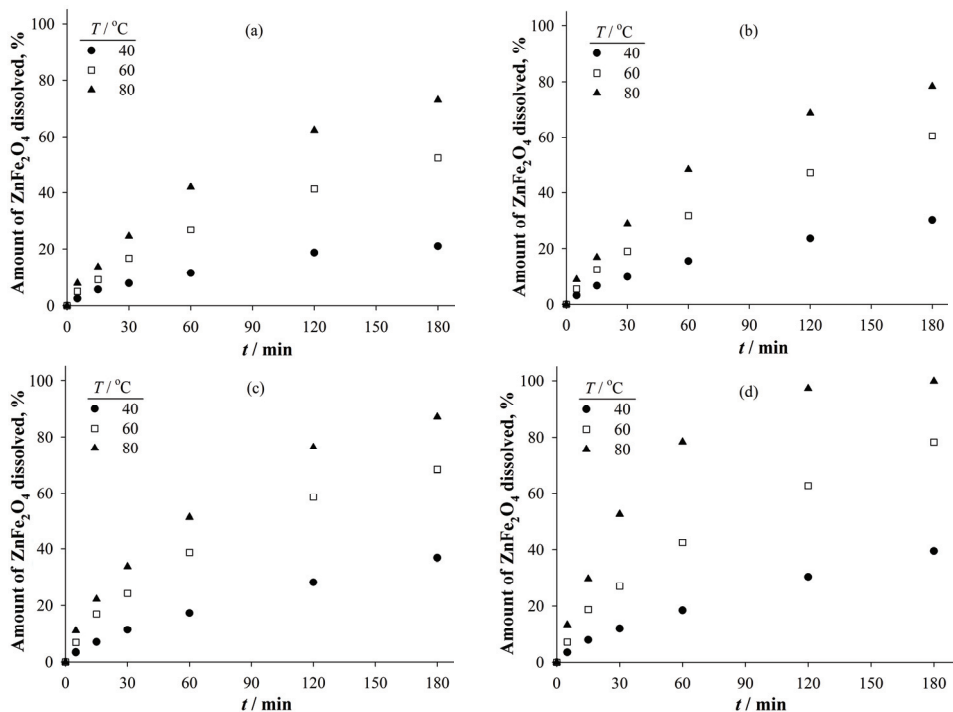


Fig. 4. ZnFe₂O₄ dissolved, content–time diagrams for different temperatures at constant HNO₃ concentration: a) 0.5, b) 1, c) 2 and d) 4 M (stirring speed: 300 rpm).

As shown in Fig. 5a–d, the dissolution of Fe₂O₃ in the EAFD was more dependent on the temperature than that of ZnFe₂O₄ and therefore the dissolution rate of Fe₂O₃ increased with increasing temperature. A dissolution of 99 % was obtained for Fe₂O₃ in the experiment performed using 4 M HNO₃ solution at 80 °C and a stirring speed of 300 rpm (Fig. 5d). However, obtaining high dissolution

rates for Fe together with Zn results in difficulties in the subsequent purification process of Zn in the leach liquor.

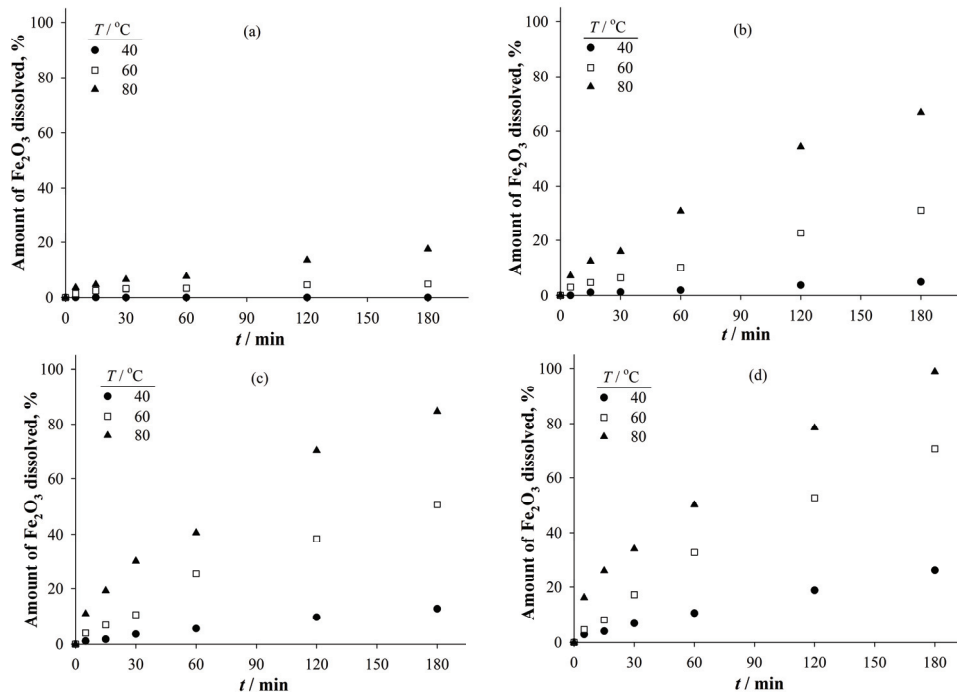


Fig 5. Fe_2O_3 dissolved–time diagrams for different temperatures at constant HNO_3 concentration: a) 0.5, b) 1, c) 2 and d) 4 M (stirring speed: 300 rpm).

A literature survey showed that H_2SO_4 solutions are generally used for the acidic leaching of EAFD. HCl solutions are not preferred due to difficulties in the electrowinning process of leach liquors since Cl_2 gas is generated. Although, it is fact that the use of H_2SO_4 solutions at moderate temperatures lowers the Fe content (1–10 %) in the leach solutions, relatively low Zn dissolution rates (about 60 %) were obtained under these experimental conditions.^{1,4,24–26} Concentrated H_2SO_4 solutions and high temperatures should be used to obtain high Zn dissolution rates. However, dissolution rate of Fe also increases rapidly in this case.

Caravaca *et al.* recovered 70.6 % of Zn and 14.5 % of Fe from EAFD using 5 M HNO_3 solution at 25 °C in 2 h and stated that the presence of zinc ferrites makes acidic leaching more attractive than alkaline leaching in terms of Zn recovery.¹¹ Although, the acidic leach liquor includes a relatively high amount of Fe compared to an alkaline leach liquor, Fe is separated from leach liquor by goethite precipitation at a pH near 2 or by solvent extraction. In this work, 93 % of Zn (100 % of ZnO and 72 % ZnFe_2O_4) and 45 % of Fe (72 % of ZnFe_2O_4 and

17.53 % of Fe_2O_3) were extracted from the EAFD in the experiment performed using 0.5 M HNO_3 solution at 80 °C.

Since the same experimental data were used for plotting the diagrams to determine the effect of the HNO_3 concentration on the dissolution rate of the EAFD in HNO_3 solutions, ZnFe_2O_4 dissolved, content-time (Fig. 6) and Fe_2O_3 dissolved, content-time (Fig. 7) diagrams are plotted only for 60 °C are shown to avoid repetition.

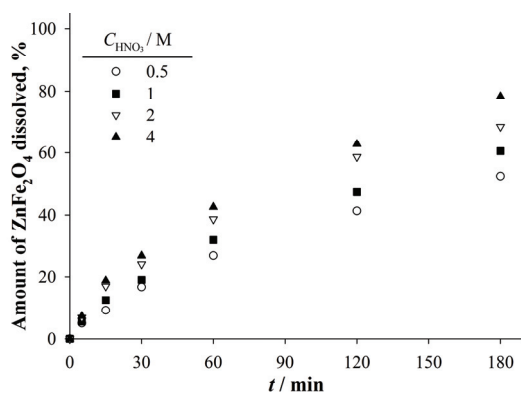


Fig. 6. ZnFe_2O_4 dissolved, content–time diagram for different HNO_3 concentrations at 60 °C.

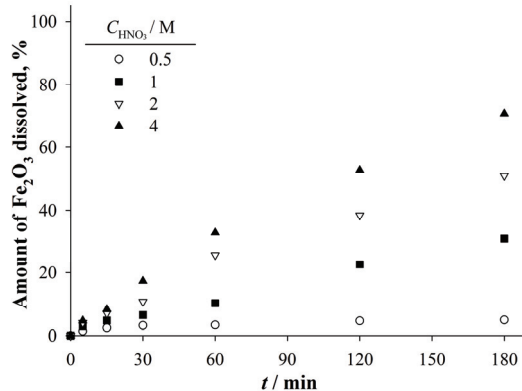


Fig. 7. Fe_2O_3 dissolved, content–time diagram for different HNO_3 concentration at 60 °C.

While the dissolution rate of ZnFe_2O_4 was not affected significantly by the increase in HNO_3 concentration at lower experimental temperatures; increasing temperature resulted in a rise in the effect of the HNO_3 concentration on the dissolution rate of ZnFe_2O_4 (Fig. 4a–d). On the other hand, the dissolution rate of Fe_2O_3 strongly depends on HNO_3 concentration and the dependency increases significantly with increasing temperature (Fig. 5a–d). Therefore, Figs. 6 and 7 show

that the dissolution rate of Fe_2O_3 is more dependent on the HNO_3 concentration than that of ZnFe_2O_4 .

SEM-EDS analysis of the EAFD and the leach residue

SEM-EDS analysis of the EAFD and the leach residue obtained from the experiment performed using 0.5 M HNO_3 at 40 °C are presented in Fig. 8a and b. It could be seen from Fig. 8a that the EAFD consisted of spherical particles with different sizes and fine agglomerated particles with irregular shapes.

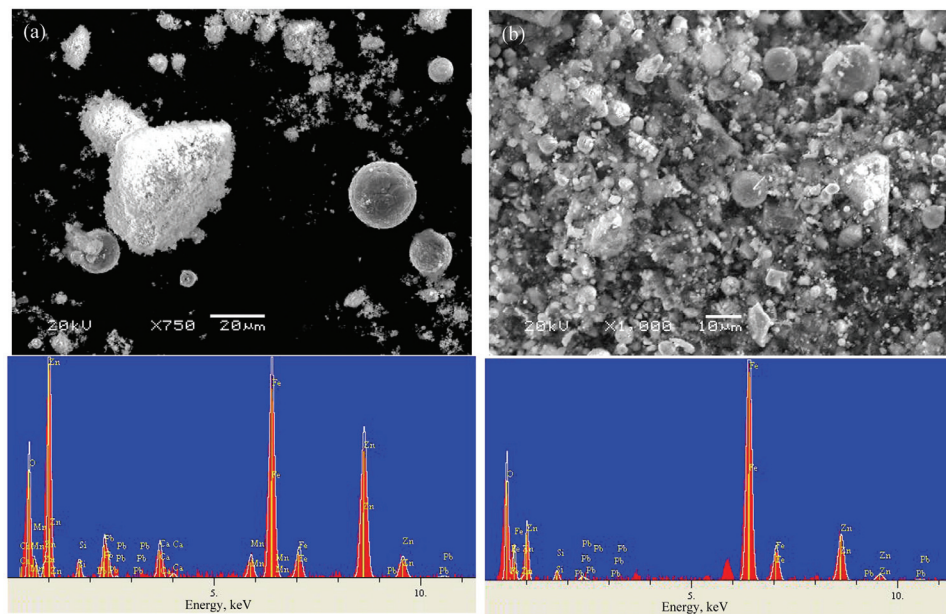


Fig. 8. SEM-EDS analysis of the EAFD and: a) the leach residue and b) obtained from the experiment performed for 180 min using 0.5 M HNO_3 at 40 °C and a stirring speed of 300 rpm.

It was determined from EDS analysis of the EAFD that the particles with spherical shape were rich in iron (Fig. 9b), whereas the particles with irregular shapes were rich in zinc and iron (Fig. 9c). These findings are in good agreement with the XRD analysis of the EAFD (Fig. 1a) and the literature.²⁷ SEM-EDS analysis of the leach residue (Fig. 8b) shows that after the leaching experiment, the particles with spherical shape become more visible and number of the particles with irregular shapes decreases due to higher dissolution rate of particles rich in zinc (ZnO and ZnFe_2O_4) than those rich in Fe_2O_3 .

CONCLUSIONS

It was determined that Fe_2O_3 was not dissolved in 0.5 M HNO_3 solution at 40 °C during a reaction time of 180 min while ZnO reacted rapidly with HNO_3 and was

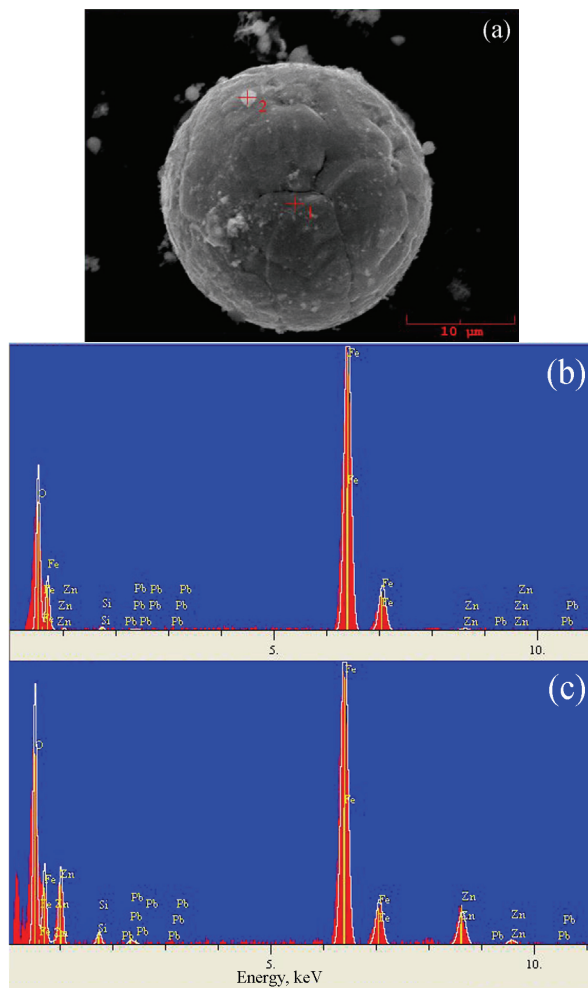


Fig. 9. EDS analysis of the EAFD.

totally dissolved in 5 min reaction time. Thus, it is possible to determine the composition of ZnO, ZnFe₂O₄ and Fe₂O₃ in the EAFD as 28.58, 37.96 and 11.33 %, respectively.

Total dissolution of the ZnFe₂O₄ was obtained from the experiments performed at 80 °C. Although, temperature is effective on the dissolution rate of both ZnFe₂O₄ and Fe₂O₃, dissolution rate of the Fe₂O₃ was more temperature dependent than that of the ZnFe₂O₄.

While the concentration of HNO₃ has slight effect on the dissolution rate of ZnFe₂O₄, the dissolution rate of Fe₂O₃ increased significantly with increasing HNO₃ concentration.

A low HNO_3 concentration (0.5 M) and high experimental temperatures (60-80 °C) should be chosen for the dissolution of the EAFD in HNO_3 solution to minimize the dissolution rate of Fe_2O_3 .

SEM-EDS analysis of EAFD showed that the Fe_2O_3 particles were spherical in shape whereas the shape of ZnO and ZnFe_2O_4 were irregular.

Acknowledgements. This work is a part of research project supported by the Scientific and Technological Research Council of Turkey (TUBITAK, Project No. 118M376). The authors would like to thank TUBITAK for financial support. This work was also supported by the Scientific Research Projects Coordination Unit of Istanbul University-Cerrahpasa (Project No. FDP-2018-31847).

ИЗВОД

ИСПИТИВАЊЕ УСЛОВА СЕЛЕКТИВНОГ ЛУЖЕЊА ZnO , ZnFe_2O_4 И Fe_2O_3 У HNO_3 ИЗ ПРАШИНЕ ЕЛЕКТРОЛУЧНЕ ПЕЋИ

MERT ZORAGA, TUGBA YUCEL, SEDAT ILHAN и AHMET ORKUN KALPAKLI

*Istanbul University-Cerrahpasa, Engineering Faculty, Metallurgical and Materials Engineering Department,
34320, Avcilar, Istanbul, Turkey*

Прашина електролучне пећи (EAFD) углавном укључује једињења која садрже Zn, Fe, Pb, Ca и Mn. Дакле, EAFD је класификован као опасан отпад. У овом раду је испитано понашање растворана једињења која садрже Zn и Fe из EAFD у растворима азотне киселине (HNO_3). Састав једињења која садрже Zn и Fe у EAFD утврђен је као 28,58 % ZnO , 37,96 % ZnFe_2O_4 и 11,33 % Fe_2O_3 . Испитан је утицај брзине мешања, температуре и концентрације HNO_3 на брзину растворана ZnO , ZnFe_2O_4 и Fe_2O_3 и утврђени су оптимални услови лужења. Док се ZnO брзо растворава, брзина растворана ZnFe_2O_4 се повећавала са повећањем температуре и концентрације HNO_3 . Fe_2O_3 није био растворљив у 0,5 M раствору Fe_2O_3 на 40 °C, док је био потпуно растворен у 4 M раствору HNO_3 на 80 °C.

(Примљено 23. маја 2020, ревидирано 16. децембра, прихваћено 17. децембра 2021)

REFERENCES

1. P. Oustadakis, P. E. Tsakiridis, A. Katsiapi, S. Agatzini-Leonardou, *J. Hazard. Mater.* **179** (2010) 1 (<https://doi.org/10.1016/j.jhazmat.2010.01.059>)
2. T. Havlik, M. Turzakova, S. Stopic, B. Friedrich, *Hydrometallurgy* **77** (2005) 41 (<https://doi.org/10.1016/j.hydromet.2004.10.008>)
3. The Union of Chambers and Commodity Exchanges of Turkey, *Turkish Ferrous and Nonferrous Metals Council Report*, 2016, <https://www.tobb.org.tr/Documents/yayinlar/EkonominRapor/Eng/2017%20Economic%20Report.pdf> (accessed 23/10/2018)
4. T. Havlik, B. De Souza, A. M. Bernardes, I.A.H. Schneider, A. Miškufová, *J. Hazard. Mater.* **135** (2006) 311 (<https://doi.org/10.1016/j.jhazmat.2005.11.067>)
5. J. R. Donald, C. A. Pickles, *Can. Metall. Q.* **35** (1996) 255 ([https://doi.org/10.1016/0008-4433\(96\)00009-2](https://doi.org/10.1016/0008-4433(96)00009-2))
6. N. Šrbac, I. Mihajlović, V. Andrić, Ž. Živković, A. Rosić, *Can. Metall. Q.* **50** (2011) 28 (<https://doi.org/10.1179/000844311X552287>)
7. M. H. Morcali, O. Yucel, A. Aydin, B. Derin, *J. Min. Metal.* **48** (2012) 173 (<https://doi.org/10.2298/JMMB111219031M>)

8. X. Lina, Z. Penga, J. Yana, Z. Li, J.Y. Hwang, Y. Zhang, G. Li, *J. Clean. Prod.* **149** (2017) 1079 (<https://doi.org/10.1016/j.jclepro.2017.02.128>)
9. V. N. R. Sarma, K. Deo, A. K. Biswas, *Hydrometallurgy* **2** (1976) 171 ([https://doi.org/10.1016/0304-386X\(76\)90026-8](https://doi.org/10.1016/0304-386X(76)90026-8))
10. M. Cruells, A. Roca, C. Núñez, *Hydrometallurgy* **32** (1992) 213 ([https://doi.org/10.1016/0304-386X\(92\)90119-K](https://doi.org/10.1016/0304-386X(92)90119-K))
11. C. Caravaca, A. Cobo, F. J. Alguacil, *Resour. Conserv. Recycl.* **10** (1994) 35 ([https://doi.org/10.1016/0921-3449\(94\)90036-1](https://doi.org/10.1016/0921-3449(94)90036-1))
12. D. K. Xia, C. A. Picklesi, *Miner. Eng.* **13** (2000) 79 ([https://doi.org/10.1016/S0892-6875\(99\)00151-X](https://doi.org/10.1016/S0892-6875(99)00151-X))
13. Z. Youcai, R. Stanforth, *Miner. Eng.* **13** (2000) 1417 ([https://doi.org/10.1016/S0892-6875\(00\)00123-0](https://doi.org/10.1016/S0892-6875(00)00123-0))
14. N. Leclerc, E. Meux, J. M. Lecuire, *Hydrometallurgy* **70** (2003) 175 ([https://doi.org/10.1016/S0304-386X\(03\)00079-3](https://doi.org/10.1016/S0304-386X(03)00079-3))
15. T. Havlik, B. Friedrich, S. Stopic, *World Metal. – ERZMETALL* **57** (2004) 83 (http://www.metallurgie.rwth-aachen.de/new/images/pages/publikationen/havlik_erzmetall_57_id_9401.pdf)
16. S. Kelebek, S. Yoruk, B. Davis, *Miner. Eng.* **17** (2004) 285 (<https://doi.org/10.1016/j.mineng.2003.10.030>)
17. G. Orhan, *Hydrometallurgy* **78** (2005) 236 (<https://doi.org/10.1016/j.hydromet.2005.03.002>)
18. A. J. B. Dutra, P. R. P. Paiva, L. M. Tavares, *Miner. Eng.* **19** (2006) 478 (<https://doi.org/10.1016/j.mineng.2005.08.013>)
19. R. A. Shawabkeh, *Hydrometallurgy* **104** (2010) 61 (<https://doi.org/10.1016/j.hydromet.2010.04.014>)
20. F. Kukurugya, T. Vindt, T. Havlik, *Hydrometallurgy* **154** (2015) 20 (<https://doi.org/10.1016/j.hydromet.2015.03.008>)
21. N. Peng, B. Peng, H. Liu, D. H. Lin, K. Xue, *Can. Metall. Q.* **56** (2017) 301 (<https://doi.org/10.1080/00084433.2017.1343174>)
22. R. L. Nyirenda, *Miner. Eng.* **4** (1991) 1003 ([https://doi.org/10.1016/0892-6875\(91\)90080-F](https://doi.org/10.1016/0892-6875(91)90080-F)).
23. B. Boyanov, A. Peltekov, K. Ivanov, *Int. J. Chem. Mol. Eng.* **9** (2015) 765 (<https://publications.waset.org/10002705/pdf>)
24. Š. Langová, J. Riplová, S. Vallová, *Hydrometallurgy* **87** (2007) 157 (<https://doi.org/10.1016/j.hydromet.2007.03.002>)
25. Z. Sedláková, D. Orac, T. Havlik, *Acta Metall. Slovaca* **12** (2006) 338 (<https://www.censo.fmmr.tuke.sk/content/clanky/200606.pdf>)
26. T. Havlik, F. Kukurugya, D. Orac, L. Parilak, *World Metal. – ERZMETALL* **65** (2012) 48 (https://www.researchgate.net/publication/279701830_Acidic_leaching_of_EAF_steelmaking_dust)
27. M. C. Da Silva, A. M. Bernardes, C. P. Bergmann, J. A. S. Tenório, D. C. R. Espinosa, *Ironmak. Steelmak.* **35** (2008) 315 (<https://doi.org/10.1179/030192307X232936>).